Pharm Res (2012) 29:983–993
DOI 10.1007/s11095-011-0638-8

RESEARCH PAPER

Detecting a Secreted Gastric Cancer Biomarker Molecule by Targeted Nanoparticles for Real-Time Diagnostics

Elena Khazanov • Eylon Yavin • Amit Pascal • Aviram Nissan • Yvonne Kohl • Meike Reimann-Zawadzki • Abraham Rubinstein

Received: 21 October 2011 / Accepted: 21 November 2011 / Published online: 10 December 2011

ABSTRACT

Purpose A real time detection of gastric cancer-associated biomarker molecules in the lumen of the stomach could assist in early detection of this multi-step malignancy.

Methods Employing α1-antitrypsin precursor (A1AT) as a secreted biomarker model, a platform with immunoassay capabilities, comprising sensing and detecting compartments was developed. It was made of a microarray-type functionalized glass, containing a high density of amine groups. Trypsin, the capturing moiety, was immobilized to the glass surface with the aid of a PEG-based spacer mixture, identified as being crucial for both capturing and detecting properties. The detecting compartment contained near infrared fluorescently labeled nanoparticles conjugated to A1AT-specific antibodies, aimed at generating an optical signal, detectable by a conventional endoscope or a video capsule.

Results The specific recognition reaction between the captured A1AT and the immuno-nanoparticles generated a profound fluorescence with a signal to noise ratio (SNR) of 12–32, in a biomarker-concentration dependent manner. Moreover, the optical recognition signal was intense enough to be detected by a video capsule simulator (with optical detection capabilities of a video capsule) with a SNR of 6–20.

Conclusions This platform could serve as a real time diagnostic kit for early detection of a *secreted* biomarker of gastric cancer.

KEY WORDS fluorescent immuno-nanoparticles · gastric cancer · human α1-antitrypsin-precursor · non-invasive imaging · protein immobilization

ABBREVIATIONS

A1AT	human α1-antitrypsin precursor
Ab	antibody
AFM	atomic force microscopy
DSC	N,N′-disuccinimidyl carbonate
FluoNP	fluorescent nanoparticles
IgG	immunoglobulin
NHS	N-hydroxy-succinimide
NHS-^{2K}PEG	O-[(N-succinimidyl)succinyl-aminoethyl]-O′-methylpolyethylene glycol 2,000
NHS-^{3K}PEG-NHS	O,O′-bis[2-(N-succinimidyl-succinylamino)ethyl]polyethylene glycol 3,000
NHS-^{5K}PEG-MAL	α-[(3-maleimido-1-oxopropyl) aminopropyl-ω-(succinimidyloxy carboxy) polyoxyethylene glycol 5,000
NIR	near infra red
NP	nanoparticles
OVA	ovalbumin

E. Khazanov • E. Yavin • A. Rubinstein (✉)
Faculty of Medicine, the School of Pharmacy Institute
for Drug Research, The Hebrew University of Jerusalem
P.O.Box 12065, Jerusalem 91120, Israel
e-mail: avrir@ekmd.huji.ac.il

A. Pascal
Given Imaging
P.O.Box 258, Yoqneam 20692, Israel

A. Nissan
Surgical Oncology Laboratory, Department of Surgery
Hadassah-Hebrew University Medical Center
Mount Scopus, P.O.Box 24035, Jerusalem 91240, Israel

Y. Kohl • M. Reimann-Zawadzki
Fraunhofer-Institut füt Biomedizinische Technik
St. Ingbert 66386, Germany

E. Yavin • A. Rubinstein
David R. Bloom Center of Pharmacy
The Hebrew University of Jerusalem
Jerusalem, Israel

PBST	PBS containing 0.05% Tween 20
PEG	polyethylene glycol
SGF	simulated gastric fluid USP
SMSA	SupermMask® SuperAmine 2
SNR	signal to noise ratio

INTRODUCTION

Gastric carcinoma, a worldwide leading cause of cancer-related death with the highest incidence in the Far East, Eastern Europe and South America, is treated by radical surgery and palliative or adjuvant chemotherapy (1,2). Although it is commonly agreed that early diagnosis is crucial for maximizing the efficacy of the medical treatment of the disease, large-scale early diagnosis programs are feasible in one high-risk country only, Japan (1,3). In Western countries, screening endoscopy has never been adopted even in high prevalence areas. Thus, gastric cancer screening, based on real-time *in-vivo* analysis of gastric fluid-born biomarkers, could serve as an attractive methodology for the detection of early stage gastric carcinoma. This could be done by probing gastric fluids by an endogastric capsule (4). An *in situ* analysis of gastric fluids during endoscopic examination could serve as an alternative approach. This could be done by a video capsule such as the Pillcam® device. Its ability to transmit high resolution images of the upper gastrointestinal (GI) epithelium (5,6) could be further elaborated for the detection of fluorescence-derived specific reactions with typical biomarker molecules.

In a previous study (7) we described a polymeric system (polyHEMA) designed for the specific recognition of α1-antitrypsin precursor (A1AT) after being captured by immobilized trypsin. In the present report we suggest an improved diagnostic system, in which the polyHEMA surface is replaced with a microarray-type functionalized glass (8). This microarray is comprised of a topological surface of low intrinsic fluorescence, high optical clarity and high density of functional NH_2 groups (9). The transparency of this system is crucial for transmitting the expected specific fluorescence signal back into a detector mounted underneath. The chemically active surface is utilized for grafting PEG-based spacers for the purpose of increasing the recognition capabilities. Furthermore, such spacers are expected to reduce non-specific adsorption of biological matter.

In order to amplify the optical immunosensing detection signal (10), the ELISA-like recognition machinery that typically employs fluorescently labeled antibodies was replaced by nanoparticles (FluoNP) (11) containing a fluorophore in the near infra red (NIR) range. Such NIR labels have the advantage of generating minimal tissue background fluorescence (12). To eventually detect the biomarker, FluoNP were modified with antibodies specific to A1AT.

Microarray platforms have been used extensively in the past for identifying protein expression, protein–protein interactions and molecular patterns as disease "biosignatures" (13). Inasmuch, ELISA microarray technology is used to quantify proteins (14,15) by employing different methods. For example, BSA-*N*-hydroxysuccimide (BSA-NHS) was used to covalently bind proteins to a platform surface, rendering it accessible to macromolecules in the examined medium (8).

The goals of this study were to immobilize trypsin to a microarray-type glass surface by a series of PEG-based spacers and capture A1AT to the immobilized enzyme; conjugate A1AT antibody (A1AT Ab) to the surface of fluorescently tagged NP; assess the ability of this newly created A1AT immunosensor to recognize captured A1AT; examine if the derived surface fluorescence can be detected *in vitro*, in a concentration-dependent manner, by a low-sensitivity optical device with the optical capabilities of a video pill; and gear towards *in vivo* testing of the immunosensor device and test its biocompatibility.

MATERIALS AND METHODS

Materials

Proteins

Alexa-fluor 555 labeled ovalbumin (OVA) was purchased from Molecular probes (Eugene, OR, USA); trypsin from bovine pancreas (≥10,000 BAEE units/mg protein) and human α1-antitrypsin precursor (A1AT) were purchased from Sigma (St Louis, MO, USA).

Antibodies

Alexa-fluor 568 and 647 (secondary Ab) labeled goat anti-rabbit IgG (h+l) were purchased from Molecular Probes (Eugene, OR, USA); anti rabbit HRP-conjugated IgG and rabbit anti human A1AT IgG (primary Ab) were purchased from Sigma (St Louis, MO, USA).

Spacers

N,*N*′-disuccinimidyl carbonate (DSC), O-[(n-succinimidyl) succinyl-aminoethyl]-O′-methylpolyethylene glycol 2,000 (NHS-^{2K}PEG) and O,O′-bis[2-(*N*-succinimidyl-succinylamino)ethyl]polyethylene glycol 3,000 (NHS-^{3K}PEG-NHS) were purchased from Sigma (St Louis, MO, USA).

α-*N*-[(3-maleimido-1-oxopropyl)aminopropyl-ω-(succinimidyloxy carboxy), polyoxyethylene glycol 5,000 (NHS-^{5K}PEG-MAL) and NHS-^{5K}PEG were purchased from NOF (Tokyo, Japan). 4,4′-Dithiopyridine (DTDP); *N*-succinimidyl 3-(2-pyridyldithio)propionate (SPDP) and 3,3′,5,5′-tetramethylbenzidine (TMB reagent) were purchased from Sigma (St Louis, MO, USA).

Supermask Superamine® 2 (SMSA) glass slides, partitioned into 24 wells, possessing ultra-low intrinsic fluorescence and background noise, containing 2×10^{13} surface amino groups/mm^2, were purchased from Arrayit, Sunnyvale (CA, USA).

Optical simulator, equipped with a low power laser source, uncooled small silicone detector, a lock-in amplifier, and appropriate filters, mimicking the detection capability of an endoscopic video pill was provided by Given Imaging, Yoqneam, Israel.

Fluorescent Nanoparticles (FluoNP)

Carboxylate-modified polystyrene nanoparticles (Fluospheres®, 200 nm) labeled with boradiazaindacene (BODIPY, 660–680) were purchased from Molecular Probes (Eugene, OR, USA).

All solvents were analytical grade.Water was purified by reverse osmosis.

Cell Cultures

Caco2 cells (human colon adenocarcinoma cells, ATCC 169, DSMZ GmbH, Braunschweig, Germany) were cultivated in Dulbecco's MEM/Nut Mix F-12 (HAM) medium supplemented with 20% fetal calf serum and 1% penicillin/streptomycin (Invitrogen, Karlsruhe, Germany). L929 cells (from mouse connective tissue, ATCC, DSMZ, Germany) were cultivated in RPMI 1680 medium (Invitrogen, Karlsruhe, Germany) supplemented as above.

Proteins Thiolization

The PyMOL molecular modeling software (DeLano Scientific LLC, CA, USA) was used to assess the number of available cysteine molecules on the surface of trypsin and OVA, in order to evaluate the potential of either of the proteins to interact with maleimide moieties presented in the PEG spacers. According to this analysis, trypsin had no surface cysteines but six internal S–S bonds, while OVA had four buried sulfhydryls and one S–S bond.

To allow the heterobifunctional NHS-^{5K}PEG-MAL spacer to react with the proteins used in this study (trypsin or Alexa Fluor 555 labeled OVA), proteins were thiolated (16) by mixing 0.1 mg of either protein with a 200-fold molar excess of *N*-succinimidyl-3-(2-pyridyldithio) propionate (SPDP) for 30 min at RT. Unreacted SPDP was removed by centrifugation (14,000 rpm, 30 min, RT) in Microcon YM-10 ultrafiltration test-tubes equipped with a 10 kDa cut-off, low-binding, hydrophilic cellulose membrane (Millipore, Billerica, MA, USA). The protein-SPDP complex was then reduced with 1 mM of dithiothreitol (DTT) (30 min in PBS pH 7.4, 2 mM EDTA, RT) under N_2, after which DTT was removed by filtration (Microcon YM-10 as above). The thiolated trypsin and OVA were re-suspended in PBS, pH 6.5 and stored at −20°C until use.

The amount of sulfhydryl groups in the thiolated proteins was determined by the DTDP method (17). Samples of the thiolated proteins were diluted with PBS pH 6.5 to a final volume of 200 μL (estimated final sulfhydryl concentration of ~40 μM). The pH was adjusted to 7.0 by the addition of 40 μL of NaH_2PO_4 (100 mM) and 0.2 mM of EDTA. After the addition of 10 μL of 4 mM 4,4′-dithiodipyridine (DTDP) reagent, the mixture was immediately vortexed, and after 5 min incubation at RT, its absorbance was measured at 324 nm against a blank buffer. The amount of sulfhydryl groups in the tested proteins was calculated employing 4-thiopyridone ($\varepsilon=21400$ M^{-1} cm^{-1} at $\lambda=324$ nm) as a standard.

Grafting the SMSA Glass Slides with Spacer Arms and the Subsequent Protein Attachment

In separate experiments SMSA surfaces were grafted with one of the following spacer arms: (*a*) the homobifunctional, DSC, (*b*) the homobifunctional NHS-^{3K}PEG-NHS, (*c*) a mixture of NHS-^{3K}PEG-NHS and ^{2K}PEG-NHS and (*d*) the heterobifunctional MAL-^{5K}PEG-NHS (Scheme 1).

N-hydroxy-succinimide (NHS) PEG derivatives were used as this chemistry allows facile attachment of the spacers to the SMSA surface. The monofunctional NHS-^{2K}PEG and NHS-^{5k}PEG spacers were used as controls due to their expected *ability* to bind to the SMSA surface and *inability* to bind the protein probes (trypsin, OVA or IgG). In general, the ability of the spacer-modified SMSA surfaces to interact with proteins was examined by their incubation (1 h, 25°C) with increasing concentrations of Alexa Fluor 555 labeled OVA (1–50 μg/ml) or Alexa Fluor 568 labeled IgG (25–100 μg/ml) in PBS, pH 7.4. Unbound proteins were removed by rinsing with PBS containing 0.05% w/v Tween 20 (PBST). The extent of protein binding was determined fluorometrically in a GenePix Pro 4000 microarray scanner (Axon Instruments, CA, USA).

Grafting SMSA with the Homobifunctional Spacers Followed by Trypsin Immobilization

SMSA wells were incubated for 1 h (at 25°C) with 30 mM of DSC or 30 mM of NHS-^{3Kk}PEG-NHS or a mixture of 10 mM of NHS-^{3K}PEG-NHS with 50 mM of NHS-^{2K}PEG

Scheme 1 The various spacers used to graft trypsin to the SMSA surfaces (*thick line* at the left of each molecule): (**a**) *N,N′*-Disuccinimidyl carbonate (DSC); (**b**) O,O′-bis[2-(N-succinimidylsuccinylamino) ethyl] polyethylene glycol 3,000 (NHS-^{3K}PEG-NHS); (**c**) a mixture of NHS-^{3K}PEG-NHS and O-[(N-succinimidyl)succinyl-aminoethyl]-O′-methylpolyethylene glycol 2,000 (NHS-^{2K}PEG); (**d**) *α*-N-[(3-maleimido-1-oxopropyl)aminopropyl-*ω*-(succinimidyloxy carboxy), polyoxyethylene glycol 5,000 (^{5K}PEG-NHS-MAL).

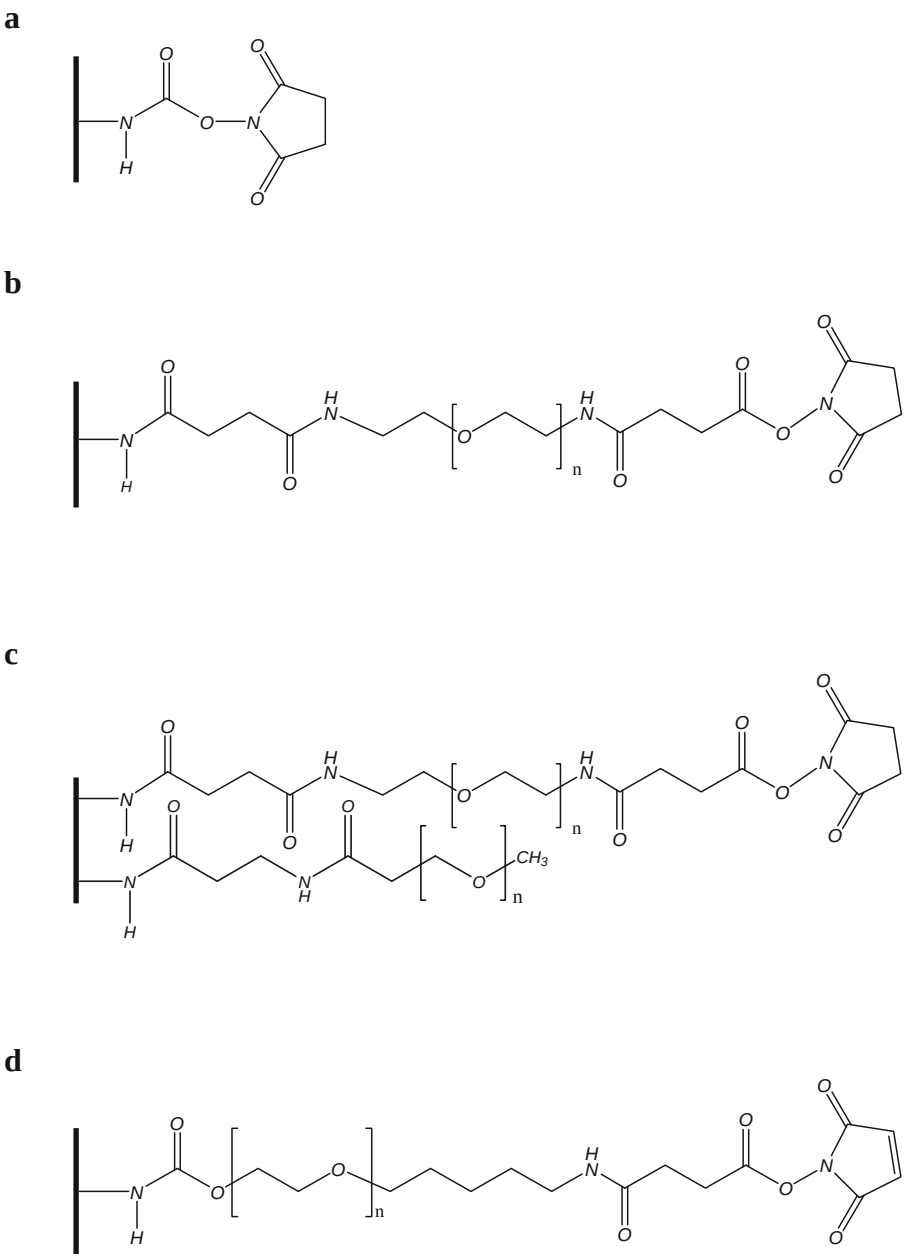

in 45 mM phosphate/10 mM borate buffer (pH 8.5). A PBS rinse was used to remove physically adsorbed spacer residues. Trypsin (200 μg/ml in PBS, pH 5) was then added to each well and incubated (1 h, RT), followed by a PBST rinse to remove unbound trypsin residues. To block unbound spacer ends the wells were then incubated with 1% BSA followed by glycine buffer (30 mM glycine, 1 mg/ml NaN_3, 0.1 mg/ml Tween 85, pH 8.8).

Grafting the SMSA with the Heterobifunctional NHS-^{5K}PEG-MAL Spacer Followed by Thiolated Trypsin Immobilization

The SMSA wells were incubated (1 h, 25°C) with 20 mM of NHS-^{5K}PEG-MAL in PBS (pH 7.4). A PBS rinse was used to remove physically adsorbed spacers residues. Thiolated trypsin (200 μg/ml in PBS, pH 5) was then added to the wells and incubated (1 h, RT). Unbound thiolated trypsin was removed by washing with PBST. Unbound spacer ends were blocked with 1% BSA.

Atomic Force Microscopy (AFM)

The surface of SMSA glass slides onto which trypsin or thiolated trypsin was immobilized with the aid a mixture of NHS-^{3K}PEG-NHS and PEG-^{2K}NHS or with NHS-^{5K}PEG-MAL was examined by a Dimension 3100 microscope equipped with a Nanoscope V controller (Veeco, CA, USA). The AFM images were recorded in a

tapping mode at 25°C. A commercial silicon tip (rotated to optimize sidewall angle symmetry) was used with a resonance frequency (f) of 300 kHz and a spring constant (k) of 50 Nm^{-1}. The AFM analysis was repeated twice in different SMSA wells (three different locations, chosen randomly) for each type of immobilized protein. Images were processed using NanoScope software (Digital Instruments/ Veeco Metrology Group).

Ab Coupling to the FluoNP

The FluoNP (9.2×10^{11} particles/200 µl) were activated by their mixing with 10 mg of sulfo-NHS and 5 mg of EDAC in PBS (10 mM, pH 7.0) for 15 min (18). Unreacted reagents were removed by centrifugation (14,000 rpm 12 min) and rinsed with a carbonate buffer (10 mM, pH 8.5).

The fraction containing the activated FluoNP was collected and re-suspended (Labsonic U tip sonicator) in 100 µl of the carbonate buffer. Coupling of the activated FluoNP with the secondary Ab (goat anti-rabbit IgG) was accomplished by a 3 h mixing of 200 µg of the Ab with the activated FluoNP in PBS, after which the conjugated microspheres were rinsed with a glycine buffer twice (14,000 rpm, 30 min, 4°C). Remaining active groups and unreacted regions on the FluoNP surface were blocked by storing the goat anti-rabbit IgG-coupled FluoNP in a glycine buffer containing 10 mg/ml of BSA, at 4°C. Before use, the FluoNP were mixed thoroughly and sonicated to break possible aggregates. IgG–FluoNP conjugation efficiency was determined fluorometrically by using of the Alexa Fluor 488-labelled Ab (Fig. 1). The FluoNP-conjugates properties are summarized in Table I.

Functional Analysis of the Detection System

The studies were conducted in the modified SMSA wells. Each well contained 50 µl of simulated gastric fluid USP (SGF) or aspirated gastric contents. Gastric contents were obtained from human subjects undergoing elective gastrointestinal surgery for reasons other than gastric cancer. The study protocol was reviewed and approved by the Independent Ethical Committee of the Hadassah-Hebrew University Medical Center (Helsinki Committee, protocol #0524-08-HMO). Gastric fluids were buffered with a bicarbonate buffer (3.5 mM $NaHCO_3$ and 0.8 mM citric acid, pH 8.5) and spiked with increasing concentrations (0–100 µg/ml) of A1AT. After 1 h incubation at 37°C and a PBS rinse, rabbit polyclonal anti-human A1AT (first Ab) was added to each well, incubated (60 min, 37°C) and rinsed. In separate studies either 75 µg/ml of secondary Alexa Fluor 647-labeled goat anti-rabbit IgG, or 1.8 mg/ml of the FluoNP, coupled to goat anti-rabbit IgG (20–30 µg/ml) were added to each well and incubated (37°C, 60 or 30 min, respectively). Unbound IgG or IgG–FluoNP conjugates were removed by PBST rinse. Fluorescent intensity was measured by the GenePix Pro 4000 microarray scanner.

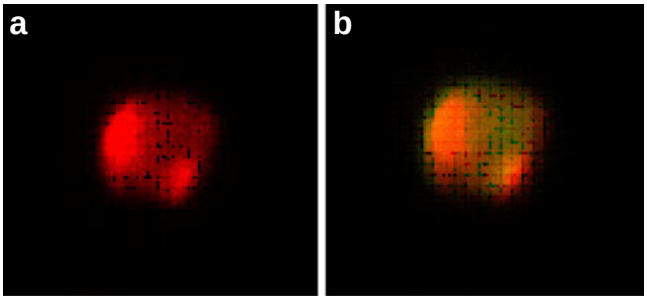

Fig. 1 Confocal laser scanning microscope (CLSM) images (x252) of two fluorescent NP in 1% agarose gel. (**a**) Two 200 nm NP labeled with BODIPY-660-680; (**b**) overlapped images of **a** after coupling with the Alexa Fluor 488®-labeled -goat anti-rabbit IgG.

The use of FluoNP coupled to the goat anti-rabbit IgG for the A1AT detection allowed us to decrease the photomultiplier tube (PMT) intensity from 500 to 290 for obtaining a comparable fluorescent signal by the microarray scanner.

Cytotoxicity Assessment of the Modified SMSA Glass Slides

Since this platform was designed for real-time gastric cancer detection (after insertion into an endoscopic device), possible cytotoxicity of the SMSA glass slides was preliminarily assessed after conjugation to 30 mM of either NHS-^{2K}PEG-NHS spacer or DSC linker. This was conducted by the BrdU cell proliferation assay and by viable count. Naked (unmodified) SMSA glass slides served as a control.

BrdU Assay (Roche, Mannheim, Germany)

The conjugated SMSA glass sides were crushed to a fine powder, added to each cell culture medium and shaken for 24 h. The Caco-2 or the L929 cells were seeded, separately, in 96 well-microplates (10^4 cells/100 µl/well) and cultivated over 24 h. The incubation medium was then replaced by the medium incubated with the crushed SMSA. Triton X-100 2% was used as a positive control. After an additional incubation (24 h, 37°C), 10 µl of BrdU labeling solution was added to each well to obtain a final BrdU concentration of 10µM. To quantify the cellular proliferation rate, the developed absorbance in each well was monitored in a microplate ELISA-reader (Tecan Deutschland, Crailsheim, Germany) at 450 nm (reference wavelength 690 nm).

Table I Characterization of the FluoNP-conjugates with Secondary Ab

Final number of FluoNP/ml dispersion	4×10^{12}[a]
Number of dye (BODIPY, 660–680) molecules/single FluoNP	1.1×10^{5}
Number of dye (BODIPY, 660–680) molecules/ml dispersion	4.4×10^{17}
Number of dye molecules used for the detection/42 mm^2 slide well	2.4×10^{15}
Ab bound to a single FluoNP (μg/ml)	20–30[b]
Number of Ab molecules/single FluoNP	~100–150

[a]FluoNP recovery after Ab conjugation: 85%

[b]Ab recovery: 10–15%

Direct Contact Assay

In this study cells (2,500 per well) were seeded on the modified SMSA. After incubation (24 h, 37°C) the cell culture medium was replaced with 1 ml of a dye solution composed of fluorescein diacetate (30 µg/ml) and propidium iodide (40 µg/ml) for a short 15 s incubation. After washing the cells with PBS the amount of viable and dead cells cultured on the modified SMAS was analyzed immediately by a BH2-RFCA-water immersion microscope (Olympus, Hamburg, Germany). Successively, a bright field image and two fluorescent images (470 nm and 555 nm) were taken from the same section of the sample (HV-C20 camera). In total, three separate independent sections of each sample were analyzed. The ratio of viable (emit green light at 525 nm) to dead cells (emit red light at 602 nm) was calculated using the software analysis 3.2 (Olympus, Hamburg, Germany).

RESULTS

To enable the efficient coating of the SMSA glass slide surface (bearing reactive amino moieties) with capturing molecules, a spacer molecule was employed. In a set of preliminary studies utilizing Alexa Fluor 555 labeled OVA as a protein probe, the glass surface was treated with either DSC (a short, homobifunctional linker), or the homobifunctional PEG spacer, NHS-^{3K}PEG-NHS. The magnitude of attachment of a protein probe to the glass surface was then assessed fluorometrically. The use of DSC did not increase SMSA surface reactivity towards Alexa Fluor 555 labeled OVA (Fig. 2). A profound coupling of the fluorescent protein probe was observed when the slide surface was modified with the NHS-^{3K}PEG-NHS. The successful interaction was a result of the bifunctionality of the PEG-based spacer. When the monofunctional spacer NHS-^{2K}PEG was used in a parallel control study, the binding of the protein probe to the activated SMSA surface was very low. The use of the NHS-^{3K}PEG-NHS spacer led to a decrease in non-specific binding to the surface.

The heterobifunctional MAL-^{5K}PEG-NHS spacer was also tested for its capability to prevent non-specific adsorption of protein probes onto the SMSA surface. For that purpose, two types of Alexa Fluor 555 labeled OVA were compared: a non-treated probe served to assess non-specific adsorption, while a thiolated probe served to assess specific binding. Figure 3 demonstrates that increasing the surface density of the spacer (as expressed by its elevated concentrations) by 5-folds interfered with non-specific adsorption of the non reactive Alexa Fluor 555 labeled OVA (creating an adsorption "shield"). The opposite occurred when the protein was thiolated. Increasing amounts of the latter were attached to the SMSA surface along with increased surface density of the grafted spacer. The signal to noise ratio (SNR) of the thiolated Alexa Fluor 555 labeled OVA compared with the non-treated Alexa Fluor 555 labeled OVA was 2–11, depending on the MAL-^{5K}PEG-NHS surface density.

A tapping mode atomic force microscopy (AFM) was used to assess how surface modification, followed by immobilizing the capturing moiety to the modified surface, affected the SMSA morphology (Fig. 4). In these images, surface roughness (visualized in the Z-axis) was quantified by measuring the root-mean-square (RMS). Thus, the surface of the unmodified SMSA slide glass was smooth with a RMS roughness value of 0.29 nm (Fig. 4a). Grafting the SMSA slide with the short DSC linker increased the RMS value to 0.36 nm (Fig. 4b). Reacting the SMSA surface with a mixture of the NHS-^{3K}PEG-NHS and NHS-^{2K}PEG (Fig. 4c) or with the longer heterobifunctional NHS-^{5K}PEG-MAL (Fig. 4d) increased RMS to 0.42 and

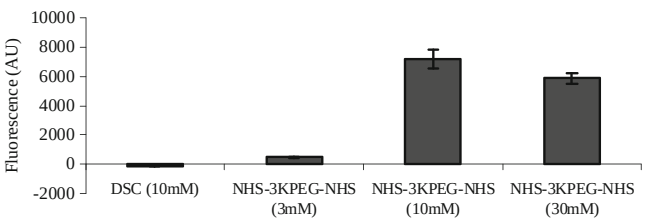

Fig. 2 Binding of Alexa Fluor 555 labeled OVA to SMSA glass slides pre-treated with either DSC linker or NHS-^{3K}PEG-NHS spacer (3, 10 and 30 mM), as analyzed by fluorescence measurements (expressed in arbitrary units) on the SMSA surface. The results were normalized to the fluorescence of non-treated (naked) SMSA, which served as a control for the DSC study, or to NHS-^{2K}PEG-treated SMSA, which served as a control for the NHS-^{3K}PEG-NHS study. Shown are the mean values of two separate experiments (performed in triplicates, altogether six replicates) ± S.D.

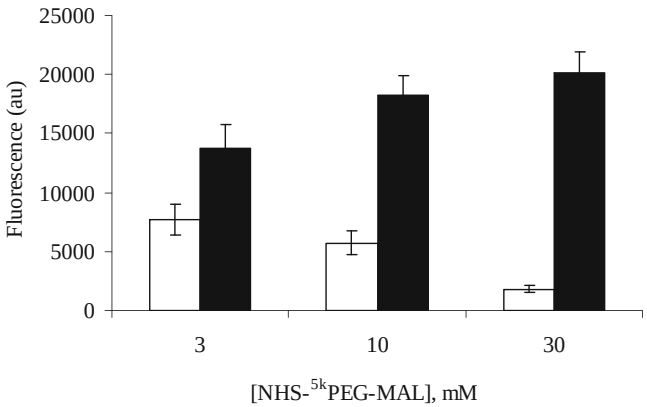

Fig. 3 The effect of thiolation of Alexa Fluor 555 labeled OVA on its binding to the surface of SMSA glass slide, pre-treated with increasing concentrations (3–30 mM) of NHS-^{5K}PEG-MAL. Empty columns: Alexa Fluor 555 labeled OVA, filled columns: thiolated Alexa Fluor 555 labeled OVA. Shown are the mean values of two experiments.

1.4 nm, respectively, with accompanied white bulges ranging from several nm to 4.37 nm (Fig. 4c) or 7.64 nm (Fig. 4d). Trypsin immobilization to the spacer mixture could be visualized by the appearance of white bulges ranging from several nm to 10.2 nm (Fig. 4e). Thiolated trypsin immobilizing to the SMSA surface with the aid of the NHS-^{5K}PEG-MAL spacer increased the RMS to 2 nm (Fig. 4f) and the bulges ranged from several nm to 19.8 nm (Fig. 4e).

A comparative study was then conducted in which Alexa Fluor 647 labeled secondary Ab and the FluoNP–Ab conjugates were compared for their potential to identify (immobilized trypsin) captured A1AT. Prior to this, non-specific binding was excluded by measuring the non-specific interaction of the two (without the addition of the primary anti A1AT specific Ab) in SGF with SMSA slides containing captured A1AT. The results are shown in Fig. 5 and demonstrate that compared to the short homobifunctional, DSC, when a mixture of the two long PEG-based spacers was used to immobilize trypsin, a significant (10- to 12-fold) decrease in the non-specific adsorption of both the fluorescent IgG and the FluoNP conjugates was observed. These results led us to employ a mixture of the homo-

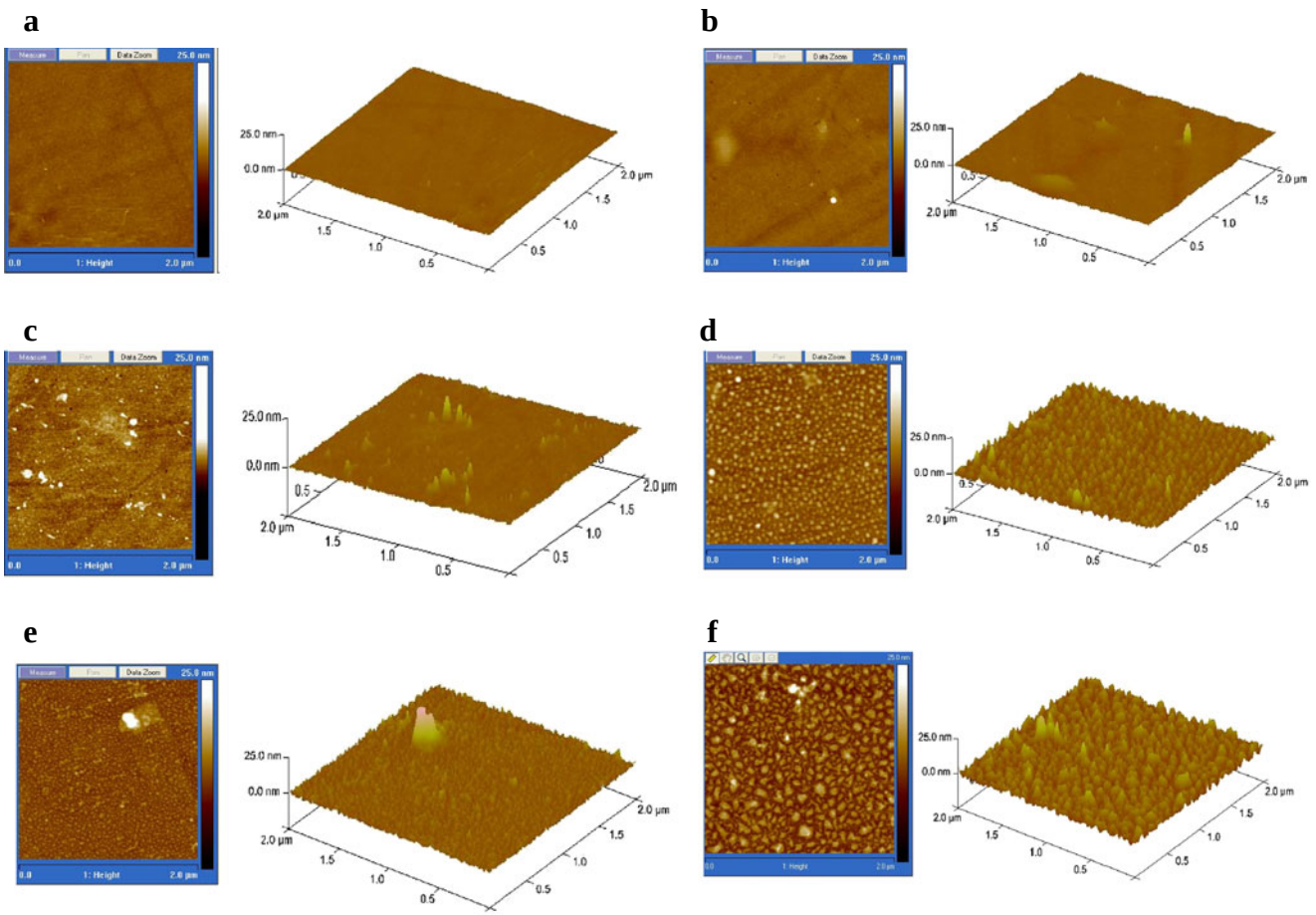

Fig. 4 Surface morphology and roughness of plain and modified SMSA slide surfaces as visualized by AFM, displayed as two- and three-dimensional images. (**a**) Untreated (naked) surface; (**b**) after DSC grafting; (**c**) after grafting with a mixture of NHS-^{3K}PEG-NHS and NHS-^{2K}PEG; (**d**) after NHS-^{5K}PEG-MAL grafting; (**e**) after trypsin immobilization via NHS-^{3K}PEG-NHS and NHS-^{2K}PEG mixture; (**f**) after thiolated trypsin immobilization via NHS-^{5K}PEG-MAL.

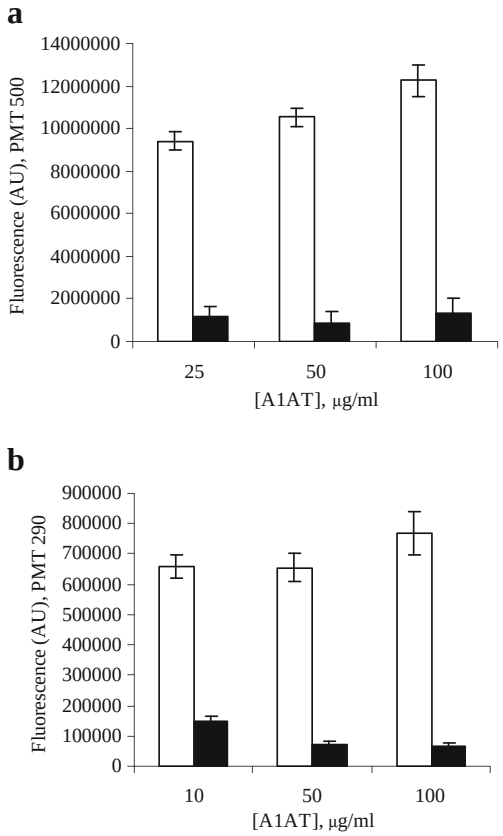

Fig. 5 Comparison of the non-specific adsorption of the Alexa Fluor 647 labeled secondary Ab (**a** at a PMT intensity 500) and the FluoNP conjugates with the secondary Ab (**b** at a PMT intensity 290) to the SMSA surface modified by the short homobifunctional linker DSC (30 mM, *empty columns*) and a mixture of the homobifunctional NHS-^{3K}PEG-NHS with NHS-^{2K}PEG spacers (10 and 50 mM, respectively, *filled columns*), used to immobilize trypsin to the surface of the SMSA slide, (both do not contain primary anti A1AT Ab). Shown are the values of three experiments ± S.D.

bifunctional and the monofunctional PEG spacers in the proceeding study in order to maximize the SNR of the captured A1AT detecting reaction.

The capability of immobilized trypsin to capture A1AT was compared to that of immobilized thiolated trypsin in SGF. Trypsin was immobilized to the surface of the SMSA slide via a mixture of NHS-^{3k}PEG-NHS and NHS-^{2k}PEG, while thiolated trypsin was immobilized via NHS-^{5K}PEG-MAL.

Quantitation of the captured A1AT was conducted by measuring fluorescence intensity employing primary and secondary, Alexa Fluor 647 labeled IgG. In a series of detection studies, conducted in SGF spiked with increasing concentrations of A1AT, it was found that immobilized trypsin enabled capturing of A1AT in a concentration-dependent manner. Compared with the non-specific adsorption to the trypsinized SMSA with no A1AT, a SNR of 12–32 (for 25–100 µg/ml of captured A1AT) was obtained (Fig. 6a).

Using identical experimental conditions, thiolated trypsin also enabled capturing of the A1AT to the SMSA surface, however, with a profoundly lower specific fluorescence and a lower SNR value of 3–7 (Fig. 6b). Therefore, the successful combination of NHS-^{3K}PEG-NHS with NHS-^{2K}PEG was employed in a subsequent study where A1AT was assessed in aspirated human gastric juice. Figure 7 shows that although detection was possible, the presence of gastric juice interfered to some extent with the detection of the captured A1AT, as indicated by the lower SNR value of 3–5.

After verifying that captured A1AT onto the SMSA surface could be detected in a sandwich ELISA-like manner, the second stage of the study was conducted, in order to increase the fluorescent detection signal in a manner that would allow detection by the optical machinery of a video capsule.

To increase the fluorescent signal derived from the specific reaction between the captured A1AT and the detecting Ab, our detection tool– Alexa Fluor 647 labeled

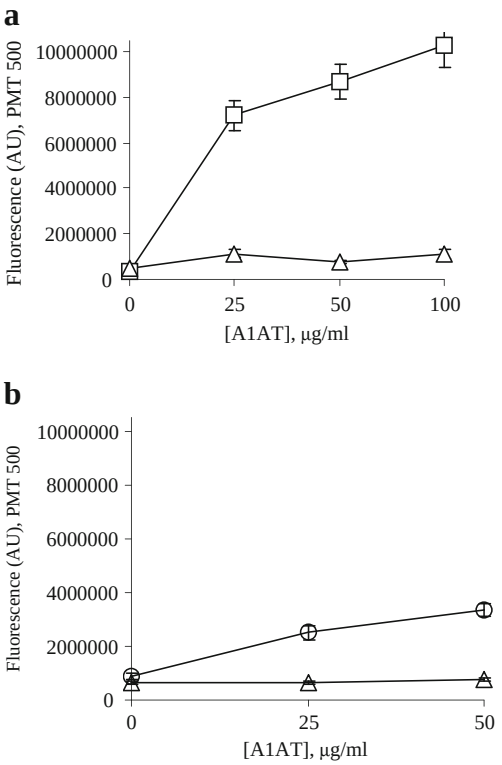

Fig. 6 Recognition and detection of captured A1AT on the surface of the SMSA slide by the primary Ab followed by Alexa Fluor 647 labeled secondary Ab in *SGF*, as expressed by fluorescence intensity. A1AT capturing was accomplished by either immobilized (via a mixture of NHS-^{3K}PEG-NHS and NHS-^{2K}PEG) trypsin (**a**), or immobilized (via NHS-^{5K}PEG-MAL) thiolated trypsin (**b**). The control system (triangles) for (**a**) was trypsin-immobilized via NHS-^{2K}PEG, while the control for (**b**) was thiolated trypsin—immobilized via NHS-^{5K}PEG. Shown are the mean values of two separate experiments, performed in triplicates (altogether six replicates) ± S.D.

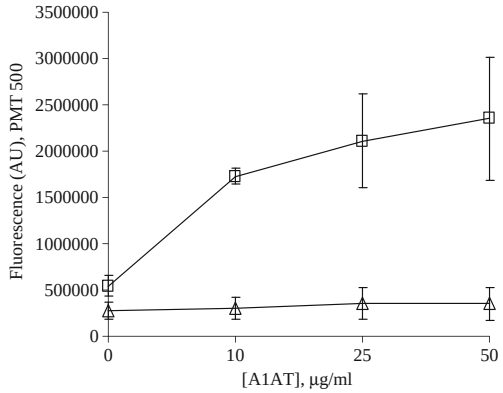

Fig. 7 Recognition and detection of captured A1AT on the surface of the SMSA slide by the primary Ab followed by Alexa Fluor 647 labeled secondary Ab in *gastric juice*, as expressed by fluorescence intensity. A1AT capturing was accomplished by immobilized (via a mixture of NHS-^{3K}PEG-NHS and NHS-^{2K}PEG) trypsin. The control system (*triangles*) comprised of a NHS-^{2K}PEG spacer through which the trypsin was immobilized to the SMSA. Shown are the mean values of five different experiments (five volunteers) ± S.D.

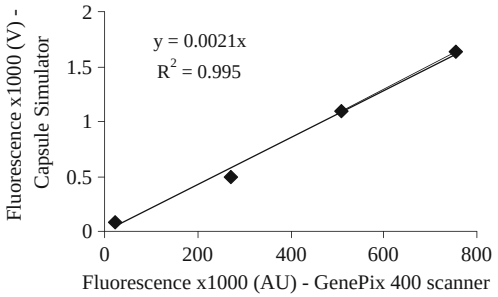

Fig. 8 The correlation between the fluorescence resulted by the specific detection reaction of the captured A1AT, on top of the SMSA slide, by the FluoNP conjugates with a secondary Ab, as measured by an array scanner (expressed by fluorescence arbitrary units) and by a video capsule simulator output (expressed in volts).

secondary Ab, was replaced with a secondary Ab conjugated to the surface of the FluoNP. The fluorescence resulted by the specific detection reaction with the captured A1AT was intensive enough to be detected by a bench capsule simulator, mimicking the capabilities of a video camera inside a remote capsule. The linear relationship between the fluorescence, as detected by the array scanner and by the bench capsule simulator, to the biomarker in SGF is shown in Fig. 8. This linearity allowed delineating a working range of A1AT of 10–100 μg/ml with a SNR value of 6–20 (Table II).

The results of *indirect* BrdU (DNA synthesis) cytotoxicity assay conducted with Caco2 and L929 cell extracts are summarized in Fig. 9. The data rules out a cytotoxic effect of the grafted spacer arms onto the SMSA slide.

The proliferation rate of both tested cell lines did not exceed that of the non-treated cells. The results of these studies involving a *direct* contact of the modified SMSA with the Caco2 and L929 cells are shown in Fig. 10 (survival analysis). Caco2 cell survival was similar for the NHS-^{3K}PEG-NHS grafted SMSA slide and the non-treated (naked) SMSA slide (77% and 86% survival, respectively). DSC grafting, however, exerted mild cytotoxicity (54% survival) to the Caco2 cells (Fig. 10a). None of the tested SMSA products was cytotoxic to the L929 cells (Fig. 10b).

DISCUSSION

In this study we showed that by immobilizing trypsin to the microarray-type activated glass, SupermMask® Super-Amine 2 (SMSA), an efficient platform for capturing A1AT was accomplished, which was then exploited for detection of the latter by immuno-FluoNP's. Trypsin grafting was achieved via functionalized PEG spacers. This was important for accomplishing covalent immobilization while maintaining trypsin functionality. Although protein immobilization to solid surfaces for biosensing applications can be accomplished by direct adsorption (19,20), a loss of up to 90% activity may occur due to experimental conditions (i.e. detection in microtiter polystyrene plates) (19,21). Thus, such an approach is limited for bench tests only.

The use of spacers, such as the PEG derivatives used in this study, for protein immobilization (22) offers remarkable flexibility with respect to terminal functionality, orientation of the recognition molecules, prevention of non-specific adsorption to the sensor surface and increased biocompatibility, due to fouling resistance of the PEG polymers (20,23).

In addition to the improved specificity obtained by introduction of the spacers (Fig. 2), a combination of the homobifunctional NHS-^{3K}PEG-NHS with the monofunctional NHS-^{2K}PEG and the heterobifunctional NHS-^{5K}PEG-MAL spacers had a profound effect on the recognition capability of the platform in terms of specificity (Fig. 3) and prevention of non-specific adsorption (Fig. 5). AFM images demonstrate how the mixture of NHS-^{3K}PEG-NHS with

Table II Detection of Increasing Concentrations of A1AT by the FluoNP as Analyzed by a Microarray Scanner (Expressed in Fluorescence Arbitrary Units) and the Bench Capsule Simulator (Expressed in Electric Potential) and Their Derived SNR Values

A1AT (μg/ml)	Fluorescence (AU x1000)	SNR	Simulator potential (V)	SNR
0	23	–	0.08	–
10	270	12	0.05	6
50	508	22	1.1	14
100	755	32	1.6	20

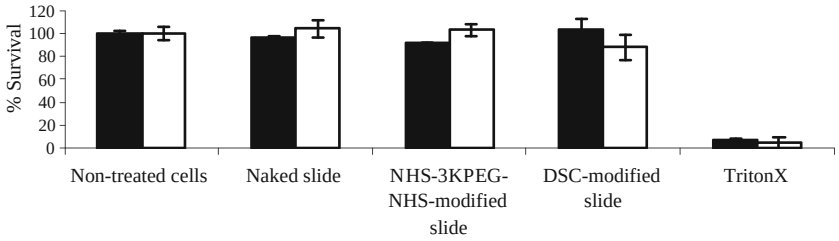

Fig. 9 Indirect cytotoxicity test (BrdU) of non-treated (naked) SMSA slides, or SMSA slides grafted, each, with 30 mM of DSC or NHS-^{3K}PEG-NHS, analyzed in Caco 2 (filled columns) or L929 (empty columns) cells. TritonX-100 (2%) was used as positive control.

NHS-^{2K}PEG (Fig. 4c) or the NHS-^{5K}PEG-MAL spacer (Fig. 4d) increased the distance between the SMSA surface and the immobilized trypsin (either native or thiolated forms, Fig. 4e and f), providing sufficient spatial freedom for the capturing and detection activities of A1AT. A series of detection studies, conducted in a simulated gastric fluid (SGF), as well as gastric juice, confirmed the importance of the PEG-based spacers (Fig. 6). Using a mixture of NHS-^{3K}PEG-NHS with NHS-^{2K}PEG and Alexa Fluor 647-labelled secondary Ab, A1AT was detected in SGF with a SNR of 22–27.

We anticipated that using thiolated trypsin would allow the use of the heterobifunctional spacer NHS-^{5K}PEG-MAL and, in turn, efficient capturing of the A1AT. However, grafting thiolated trypsin to the SMSA surface, followed by a detection analysis of the captured A1AT with the aid of Alexa Fluor 647-labelled secondary Ab, yielded an SNR value of 3 (a 7-fold reduction, Fig. 6b). This could be a result of either trypsin aggregation, which took place during the immobilization process (Fig. 4e), or the interference of the A1AT recognition sites on the modified trypsin.

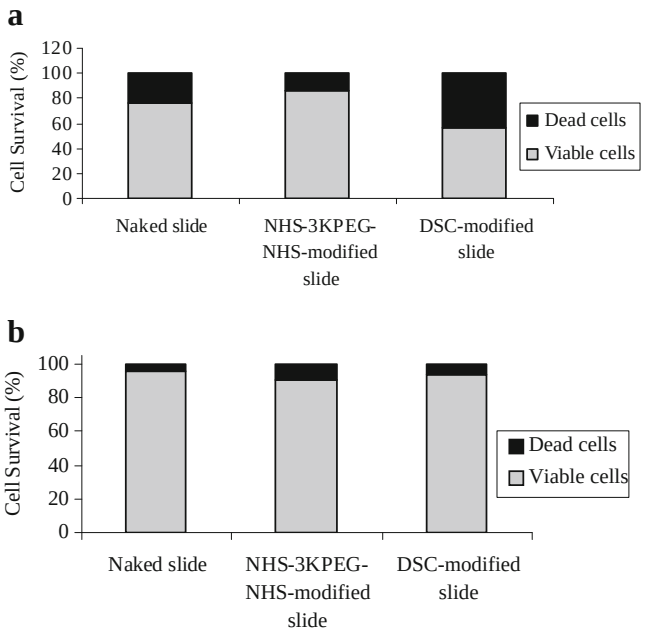

Fig. 10 Direct biocompatibility test of non-treated (naked) SMSA slides, or SMSA slides grafted, each, with 30 mM of DSC or NHS-^{3K}PEG-NHS analyzed in Caco 2 (**a**) or L929 (**b**) cells.

The success of the specific spacer mixtures NHS-^{3K}PEG-NHS and NHS-^{2K}PEG (10 and 50 mM, respectively) in enhancing A1AT capturing and detection on the SMSA platform can be related to the mixture's ability to prevent chain backfolding, thus maintaining maximal free NHS ester ends (the leaving group) accessible to the coupling reaction with trypsin. This polymer orientation is important for the creation of a "brush" assembly ("end on") rather than a "mushroom" assembly ("side-on") (24) that could be formed when the homobifunctional spacers layer is not dense enough (25). This architecture enabled the formation of optimal density of binding ends, leading to the successful grafting of trypsin or thiolated trypsin onto the SMSA surface and the consequent capturing of A1AT even in gastric juice (Fig. 7), where biological matter interferes with the detection reaction (20,26).

In this study we were interested in analyzing the specific fluorescence reaction in a bench simulator, mimicking low detection capabilities of typical diagnostic machinery such as video capsules. Indeed, we observed that optical signals, at the NIR range, that were detected easily by the GenPix 4000 scanner (Fig. 6) could not be detected by the bench (video capsule) simulator due to insufficient photonic activity on top of the SMSA surface. This led us to adopt an alternative strategy that enabled intensifying of the specific fluorescence required for the A1AT detection under real-time conditions. Instead of using a fluorescently-labelled Ab, Ab molecules were coupled to the surface of FluoNP (27,28) that, by definition, contained a higher amount of fluorescent molecules (Table I). After covalently attaching the secondary Ab to the surface of the FluoNP, the detection reaction between the captured A1AT and the immuno-FluoNP was monitored by the bench simulator. By this approach, a profound optical signal was detected in a biomarker-concentration-dependent manner (Fig. 8). Comparison between the fluorescence resulted by the specific interaction between the captured A1AT and the Ab–FluoNP conjugates to that

of captured A1AT and fluorescently-labeled Ab (Figs. 6, 8) revealed that the calculated amount of fluorescent molecules was two orders of magnitude higher when FluoNP–Ab conjugates were employed (equal to $\sim 1 \times 10^{14}$ molecues/42 mm^2 SMSA well). This amplification has led to a recognition signal 30-fold higher than the detection limit of the bench simulator, leading to the notion that the new diagnostic platform is capable of detecting A1AT at real time conditions (in SGF).

Because the SMSA glass slide was designed to detect A1AT in the lumen of the stomach (after mounting inside a video capsule), preliminary biocompatibility tests of the SMSA platforms were conducted by comparing the cytotoxicity of a naked SMSA to that of a SMSA grafted with the PEG spacer mixture. The results summarized in Figs. 9 and 10 highlight the safety of our system.

It is concluded that immobilized trypsin can capture A1AT which, in turn, can be recognized by an Ab–FluoNP conjugate. The resulted specific fluorescence could be used for the quantitative detection of A1AT in SGF and, to a lesser extent, in gastric juice by clinically used optical diagnostic machinery. This technology is being tested by our group for the real time detection of additional GI fluid-born (secreted) biomarker molecules, for the early detection of GI malignancies.

ACKNOWLEDGMENTS & DISCLOSURES

The study was supported by a research grant from the NEMO consortium of the 6th European framework program for research and technological development.

REFERENCES

1. Palli D. Epidemiology of gastric cancer: an evaluation of available evidence. J Gastroenterol. 2000;35 Suppl 12:84–9.
2. Jemal A, Siegel R, Xu J, Ward E. Cancer statistics, 2010. CA Cancer J Clin. 2010;60:277–300.
3. Tan YK, Fielding JW. Early diagnosis of early gastric cancer. Eur J Gastroenterol Hepatol. 2006;18:821–9.
4. Muretto P, Graziano F, Staccioli MP, Barbanti I, Bartolucci A, Paolini G, *et al.* An endogastric capsule for measuring tumor markers in gastric juice: an evaluation of the safety and efficacy of a new diagnostic tool. Ann Oncol. 2003;14:105–9.
5. Eliakim R, Yassin K, Shlomi I, Suissa A, Eisen GM. A novel diagnostic tool for detecting oesophageal pathology: the PillCam oesophageal video capsule. Aliment Pharmacol Ther. 2004;20:1083–9.
6. Bhuket T, Takami M, Fisher L. The use of wireless capsule endoscopy in clinical diagnostic gastroenterology. Expert Rev Med Devices. 2005;2:259–66.
7. Khazanov E, Emmanuel N, Azab AK, Barenholz Y, Yavin E, Rubinstein A. Specific detection of gastric alpha-antitrypsin by immobilized trypsin on polyHEMA films. Mol Pharm. 2010;4:944–52.
8. MacBeathand G, Schreiber SL. Printing proteins as microarrays for high-throughput function determination. Science. 2000;289:1760–3.
9. Wolter A, Niessner R, Seidel M. Preparation and characterization of functional poly(ethylene glycol) surfaces for the use of antibody microarrays. Anal Chem. 2007;79:4529–37.
10. Morgan CL, Newman DJ, Price CP. Immunosensors: technology and opportunities in laboratory medicine. Clin Chem. 1996;42:193–209.
11. Nakajima M, Takeda M, Kobayashi M, Suzuki S, Ohuchi N. Nano-sized fluorescent particles as new tracers for sentinel node detection: experimental model for decision of appropriate size and wavelength. Cancer Sci. 2005;96:353–6.
12. Adams KE, Ke S, Kwon S, Liang F, Fan Z, Lu Y, *et al.* Comparison of visible and near-infrared wavelength-excitable fluorescent dyes for molecular imaging of cancer. J Biomed Opt. 2007;12:024017.
13. Wilsonand DS, Nock S. Recent developments in protein microarray technology. Angew Chem Int Ed Engl. 2003;42:494–500.
14. Wiese R, Belosludtsev Y, Powdrill T, Thompson P, Hogan M. Simultaneous multianalyte ELISA performed on a microarray platform. Clin Chem. 2001;47:1451–7.
15. Jinand H, Zangar RC. Antibody microarrays for high-throughput, multianalyte analysis. Cancer Biomark. 2010;6:281–90.
16. Lee K, Kye M, Jang JS, Lee OJ, Kim T, Lim D. Proteomic analysis revealed a strong association of a high level of alpha1-antitrypsin in gastric juice with gastric cancer. Proteomics. 2004;4:3343–52.
17. Riener CK, Kada G, Gruber HJ. Quick measurement of protein sulfhydryls with Ellman's reagent and with 4,4′-dithiodipyridine. Anal Bioanal Chem. 2002;373:266–76.
18. Valanne A, Huopalahti S, Vainionpaa R, Lovgren T, Harma H. Rapid and sensitive HBsAg immunoassay based on fluorescent nanoparticle labels and time-resolved detection. J Virol Methods. 2005;129:83–90.
19. Kusnezow W, Jacob A, Walijew A, Diehl F, Hoheisel JD. Antibody microarrays: an evaluation of production parameters. Proteomics. 2003;3:254–64.
20. Kawaguchi T, Shankaran DR, Kim SJ, Gobi KV, Matsumoto K, Toko K, *et al.* Fabrication of a novel immunosensor using functionalized self-assembled monolayer for trace level detection of TNT by surface plasmon resonance. Talanta. 2007;72:554–60.
21. Butler JE. Solid supports in enzyme-linked immunosorbent assay and other solid-phase immunoassays. Methods. 2000;22:4–23.
22. Leckband D, Sheth S, Halperin A. Grafted poly(ethylene oxide) brushes as nonfouling surface coatings. J Biomater Sci Polym Ed. 1999;10:1125–47.
23. Uchida K, Otsuka H, Kaneko M, Kataoka K, Nagasaki Y. A reactive poly(ethylene glycol) layer to achieve specific surface plasmon resonance sensing with a high S/N ratio: the substantial role of a short underbrushed PEG layer in minimizing nonspecific adsorption. Anal Chem. 2005;77:1075–80.
24. Moghimi SM. The effect of methoxy-PEG chain length and molecular architecture on lymph node targeting of immuno-PEG liposomes. Biomaterials. 2006;27:136–44.
25. Schlapak R, Armitage D, Saucedo-Zeni N, Hohage M, Howorka S. Dense passivating poly(ethylene glycol) films on indium tin oxide substrates. Langmuir. 2007;23:10244–53.
26. Rogers KR. Recent advances in biosensor techniques for environmental monitoring. Anal Chim Acta. 2006;568:222–31.
27. Kubitschko S, Spinke J, Bruckner T, Pohl S, Oranth N. Sensitivity enhancement of optical immunosensors with nanoparticles. Anal Biochem. 1997;253:112–22.
28. Tsourkas A, Shinde-Patil VR, Kelly KA, Patel P, Wolley A, Allport JR, *et al. In vivo* imaging of activated endothelium using an anti-VCAM-1 magnetooptical probe. Bioconjug Chem. 2005;16:576–81.